



Kinematic reconstruction of vectorlike tops from fully hadronic events

Martin Stoll*

Department of Physics, University of Tokyo, Bunkyo-ku, Tokyo 113-0033, Japan

Abstract

We investigate the potential to search for the vectorlike top partner in fully hadronic final states at the LHC. An algorithm is developed which kinematically reconstructs the vectorlike top. We show that for moderate masses and a large branching fraction into top quark and Higgs boson, the reconstruction works with good quality.

Keywords: Models beyond the standard models, Top quarks, Fourth generation quarks

1. Introduction

The discovery of the Higgs boson in 2012 at the LHC [1, 2] completed the particle content of the Standard Model (SM) and triggered a new era of physics beyond the SM. As the LHC will restart soon in 2015 at $\sqrt{s} = 13\text{--}14$ TeV, it is important to explore a variety of possible scenarios that can be probed at this new energy frontier. In this paper, we discuss the possibility of searching for a vectorlike top partner and propose a new approach to reconstruct it from its decay into fully hadronic final states.

The vectorlike top partner is a heavy quark that has electric charge 2/3. It is typically assumed to mainly couple to the third-generation quarks of the SM. A variety of models predict these particles, among which are little Higgs models [3, 4] or supersymmetry with additional vectorlike matters [5].

Motivated by naturalness, the vectorlike top partner is expected to be relatively light and thus directly produced at the LHC. Previous searches gave negative results and exclusion bounds on the vectorlike top mass from $\sqrt{s} = 7$ TeV data are about 690–780 GeV from CMS [6] and 550–850 GeV from ATLAS [7, 8, 9, 10], depending on the assumed branching ratios. Searches

for pair production of vectorlike tops have been conducted for several final states available from the $t' \rightarrow th$, $t' \rightarrow tZ$ and $t' \rightarrow bW$ decay channels. In these studies, a subsequent (semi)leptonic decay is used as a typical search channel¹.

In this study, we investigate the possibility of searching for a vectorlike top partner from purely hadronic final states at the LHC, assuming that the vectorlike tops are pair-produced and dominantly decay into t and h . For a heavy vectorlike top, its decay products are considerably boosted and hence subsequent decay products of each t and h are collimated in one area of the detector. We apply substructure methods [12, 13] to identify the top quark and the Higgs boson within these large “fat” jets and propose an algorithm to determine the t - h combination based on a massive pair hypothesis. We show that for moderate masses of the vectorlike top, decent event rates are feasible within the first period of the LHC run II and find that the vectorlike top can be reconstructed with good quality.

2. Model

In this article we consider the decay of the vectorlike top (t') into top (t) and Higgs (h), which is described by

*Speaker. Email: stoll@hep-th.phys.s.u-tokyo.ac.jp

¹An exception is a recent study by CMS [11] where all-hadronic final states were investigated

the following Lagrangian²

$$\mathcal{L} = \mathcal{L}_{\text{SM}} + \bar{t}' (\iota D - m_{t'}) t' + y_t h \bar{t} t' + h.c.. \quad (1)$$

We investigate pair production of vectorlike tops at the LHC with a center-of-mass energy of 14 TeV and consider the following decay chain to fully hadronic final states:

$$pp \rightarrow t' \bar{t}', \quad (2)$$

$$t' \rightarrow th \rightarrow bjj b\bar{b}, \quad (3)$$

where j denotes u,d,c or s (anti)quarks. For simplicity, we assume that the vectorlike top decays exclusively to top and Higgs. We consider masses $m_{t'} = 800$ and 900 GeV. The top quark mass is taken to be 173.5 GeV and we assume a SM-like Higgs boson with $\text{BR}(h \rightarrow b\bar{b}) = 0.56$ for a mass of 126 GeV [14].

3. Event generation

All events are simulated with **MADGRAPH5** 1.5.14 [15] in combination with **PYTHIA** 6.4 [16] and the **DELPHES** 3 fast detector simulation [17]. The parameters of the latter are adjusted to the ATLAS detector as provided by the **MADGRAPH5** package. Common cuts are imposed on all final-state partons at generator level: transverse momentum $p_T \geq 20$ GeV and mutual separation $\Delta R \equiv \sqrt{\Delta\phi^2 + \Delta\eta^2} \geq 0.4$, where ϕ and η are the parton's azimuthal angle and its pseudorapidity.

The main background processes are $b\bar{b}b\bar{b}$, $t\bar{t}$, $t\bar{t}b\bar{b}$, and $t\bar{t}h$ after imposing all cuts described in the next section. Other processes like $b\bar{b}V$, $b\bar{b}h$, $t\bar{b} + t\bar{b}$, $b\bar{b}$, and $t\bar{t}V$ turned out negligible. Pure multijet QCD background events are difficult to simulate reliably, but we expect that they are also efficiently suppressed by our cut procedure, in particular by multiple b -tagging.

Both for signal and backgrounds, we generate events at leading order (LO) and rescale them by uniform K factors assuming the event distribution is not affected much at next-to-leading order (NLO). For signal events, the cross section is calculated at NLO using **MADGRAPH5_AMC@NLO** [15]. We obtain the K factors 1.33 for $m_{t'} = 800$ GeV and 1.32 for $m_{t'} = 900$ GeV.

We are interested in background events only in the signal region, which is defined by large scalar transverse momentum H_T at hadron level, cf. next section.

²In general, there is also a model-dependent term $\lambda h \bar{t} \gamma_5 t' + h.c.$ in the Lagrangian which can give the top quark a dominant chirality. We however expect that our results do not change significantly in the presence of this term because our algorithm is blind with respect to the chirality of the top quark. In our analysis, we assume $\lambda = 0$ for simplicity.

	SR1	SR2	SR3
H_T		≥ 1200 GeV	
tagged b		≥ 4	
tagged t	$= 1$	$= 2$	$= 2$
tagged h	$= 2$	$= 1$	$= 2$

Table 1: The signal regions. For SR1 and SR2, we demand additional conditions for reconstructing vectorlike tops (see Sec. 4.6).

For technical reasons we therefore generate events with $H_T^{\text{p.l.}} \equiv \sum_{\{\text{partons } i\}} p_T^{(i)} \geq 1000$ GeV at generator level. Alas, this parton level cut acts differently on events with different final-state multiplicity (the set of partons which contribute to the sum is different) and therefore cannot be naively applied to event generation at NLO.³

LO cross sections in the signal region are obtained by cutting on generated events.⁴ Results are then rescaled by uniform K-factors which we take as 1.40 for $b\bar{b}b\bar{b}$ [19], 1.61 for $t\bar{t}$ [20], 1.77 for $t\bar{t}b\bar{b}$ [21], and 1.10 for $t\bar{t}h$ [22]. We do not attempt to estimate uncertainties of the background cross sections, as these values should be measured experimentally from appropriate control regions. Consequently, this article does not show a cut-and-count analysis but rather demonstrates the potential of reconstructing the vectorlike top.

4. Analysis

In the following, all cuts and the kinematic reconstruction of the vectorlike top partner are explained. For a quick overview of the signal regions, see Table 1.

4.1. Scalar transverse momentum cut

In order to suppress continuum backgrounds we impose a cut on scalar transverse momentum, given by

$$H_T \equiv \sum_{\text{jets } j} p_T^{(j)} \geq 1200 \text{ GeV}. \quad (4)$$

Here and for b tagging we use the anti- k_T algorithm [23] as implemented in **FastJet** [24] with parameters $R = 0.4$ and $p_T \geq 20$ GeV for jet clustering. The vectorlike top's decay exhibits a large value of order $H_T \sim \mathcal{O}(2m_{t'})$ whereas the cross sections of all standard model processes drop exponentially.

The large H_T cut is also considered to trigger events. For the case that this is not adopted we investigated the

³For the same reason approximate methods such as MLM matching [18] are also not feasible.

⁴For better accuracy a lower cut $H_T^{\text{p.l.}} \geq 600$ GeV is imposed here.

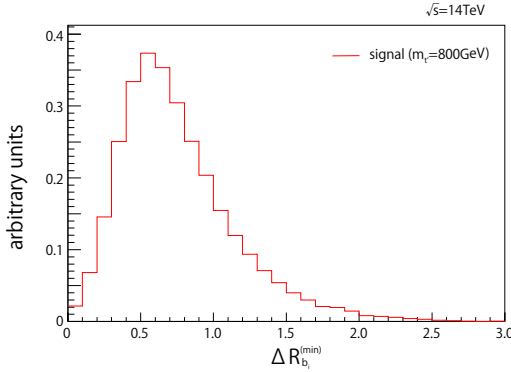


Figure 1: Distribution of bottom quark isolation for signal events (parton level). The horizontal axis corresponds to the smallest distance between each (anti)bottom quark and any other particle in the partonic final state, $\Delta R_{b_i}^{(min)} = \min_{j \neq b_i} \Delta R(b_i, j)$ ($i = 1, \dots, 6$).

following event triggers as well: 4 jets each with $p_T \geq 90$ GeV or 5 jets each with $p_T \geq 55$ GeV. Our final results do not change under these additional cuts.

4.2. Bottom tagging and cut

As the signal contains six bottom quarks in the final state, a cut on the number of b -tagged jets is indicated. b tagging is performed with an algorithm identical to the default in DELPHES [17]. We choose a working point where b -initiated jets are correctly identified with 70% probability, $\epsilon_{\text{tag}} = 0.70$, and assume the fractions of jets which are misidentified as bottom quark-initiated to be $\epsilon_{\text{mis}}^{(uds)} = 0.01$ for light jets (light quark- and gluon-initiated jets) and $\epsilon_{\text{mis}}^{(c)} = 0.10$ for charm-initiated jets.⁵

Multiple b tags cannot be treated independently unless the jets are sufficiently separated. Fig. 1 shows that this requirement holds and there is negligible jet overlap for the jet clustering radius $\Delta R = 0.4$ considered here.

We require at least 4 b -tagged jets in this analysis, which gives sufficient rejection of SM background events while retaining reasonable signal event rates.

4.3. Fat jets

For the heavy vectorlike top considered in this article, $m_r \geq 800$ GeV, its decay products t and h are typically boosted, with $p_T^{t,h} \gtrsim 200$ GeV. The final state jets emerging from the subsequent decay $t \rightarrow b jj$ (and $h \rightarrow b\bar{b}$ respectively) will therefore be collimated with

a typical distance $\Delta R_{\text{daughters}} \sim 2m_{\text{mother}}/p_T$ and can be caught within a fat jet of large radius. In this article, fat jets are clustered from calorimeter information using the Cambridge-Aachen algorithm [26, 27] with parameters $\Delta R = 1.5$ and $p_T^{\text{fat jet}} \geq 200$ GeV.

Fig. 2 shows the distribution of the smallest distance between any two of the top quarks and Higgs bosons in $pp \rightarrow t't\bar{t} \rightarrow th\bar{h}$. It is generally smaller than the fat jet radius $\Delta R = 1.5$ and thus in a typical event (at least) one fat jet contains the decay products of two partons. At least three fat jets are required as candidates for top and Higgs in SR1 and SR2 ($\sim 70\%$ of the events), and at least four in SR3 ($\sim 15\%$ of the events).

4.4. Top quark tagging and reconstruction

We rely on the HEPTopTagger [13] to tag and kinematically reconstruct boosted tops. As the concept is very similar to the our Higgs tagger implementation (see next subsection), we briefly go over the algorithm. The following procedure is applied to each fat jet.

1. First, the fat jet is successively declustered. At each step in the iterative un-doing of the last clustering of the jet j , both subjets j_1, j_2 are kept only if a substantial mass drop occurs ($\max m_{j_i} < 0.8m_j$). Otherwise the less massive subjet is removed. Subjets with $m_j < 30$ GeV are not further decomposed, which eventually ends the un-clustering stage.
2. Soft radiation is removed by applying a filtering stage and the five hardest subjets are kept.
3. A top candidate is reconstructed from three subjets if the combined mass is within $150 \leq m_{jjj} \leq 200$ GeV and various subjet mass ratios hold.⁶

⁶See Ref. [13] for a detailed discussion of these cuts. We adopt all parameters as described therein.

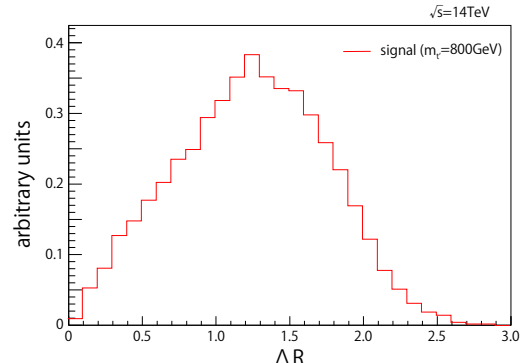


Figure 2: The smallest distance between any two of the top quarks and Higgs bosons in $pp \rightarrow t't\bar{t} \rightarrow th\bar{h}$ (parton level).

⁵For comparison the ATLAS Collaboration quotes $\epsilon_{\text{mis}}^{(uds)} \simeq 0.01$, $\epsilon_{\text{mis}}^{(c)} \simeq 0.20$ for $\epsilon_{\text{tag}} = 0.70$ at $\sqrt{s} = 7$ TeV [25] which is expected to be improved at LHC run II.

4. We require these three subjets to mutually meet the condition $\Delta R \geq 0.4$ to be consistent with a similar cut at event generation level.
5. If there are multiple top candidates, the one with a mass closest to the real top quark mass is chosen.

Note that conditions 4 and 5 are different from the original HEPTopTagger [13], to which we refer for details.

If a top candidate is reconstructed, the corresponding fat jet is not considered as Higgs candidate. In our analysis, we require 1 or 2 tagged tops in a given event.

4.5. Higgs boson tagging and reconstruction

Higgs tagging proceeds very similarly to top tagging, so we only give the modifications here. We implemented an algorithm loosely based on the BDRS Higgs tagger [12]. A comprehensive review of various tagging algorithms can be found in Ref. [28].

1. The mass-drop criterion reads $\max m_{j_i} < 0.67m_j$, and an additional symmetry requirement is imposed which reflects the splitting $h \rightarrow b\bar{b}$, $\min p_{T,j_i} / \max p_{T,j_i} > 0.09$ ⁷.
2. The filtering stage is identical to the HEPTopTagger. Note that we also keep the five hardest subjets, although in Ref. [12] it is suggested to keep only the three hardest. As a significant number of fat jets contain decay products of another t or h , our choice allows efficient tagging of those contaminated fat jets as well.
3. The mass range is $100 \leq m_{jj} \leq 150$ GeV.

4.+5. Identical to top tagging.

Unlike suggested in Ref. [12], we do not require a tagged b jet inside the reconstructed Higgs.⁸

We demand 1 or 2 reconstructed Higgs bosons in this analysis.

4.6. Massive pair hypothesis and reconstructed mass

The vectorlike top mass is kinematically reconstructed from the tagged top quark and Higgs boson,

$$M(t, h) = \sqrt{(p_t^\mu + p_h^\mu)^2}, \quad (5)$$

where p_i^μ is the four-momentum of given particle i .

In the case that both two tops (t_1, t_2) and two Higgs bosons (h_1, h_2) are reconstructed in an event (SR3),

there are two possible combinations for the vectorlike tops. For consistency we choose the combination which gives a smaller mass difference,

$$\min [|M(t_1, h_1) - M(t_2, h_2)|, |M(t_1, h_2) - M(t_2, h_1)|]. \quad (6)$$

Next, let us consider the case where one top (t) and two Higgs bosons (h_1, h_2) are reconstructed (SR1).⁹ In this case, three out of four particle momenta are known, $p_t^\mu, p_{h_1}^\mu, p_{h_2}^\mu$. Under the signal hypothesis, the momentum of the undetected fourth particle (denoted as t_{miss} with $m \equiv m_t$) obeys the following constraint,

$$\vec{p}_{T,t_{\text{miss}}} + \sum_{i=t,h_1,h_2} \vec{p}_{T,i} = 0. \quad (7)$$

To determine the unknown parameter $p_{z,t_{\text{miss}}}$, we demand the two reconstructed vectorlike tops to have equal masses. For the two combinations for $t-h$ pairs this reads

$$M(t, h_1) = M(t_{\text{miss}}, h_2), \quad (8)$$

$$\text{or } M(t, h_2) = M(t_{\text{miss}}, h_1). \quad (9)$$

The solutions of these equations constitute the pairing:

- (a) If neither of the equations gives a solution, the event is discarded.
- (b) If exactly one of the equations yields a solution, the combination of t and h is uniquely determined and we obtain $M(t, h_1)$ or $M(t, h_2)$, respectively.
- (c) If both equations give solutions we choose the $t-h$ pair where the pseudorapidity $\eta_{t_{\text{miss}}}$ is minimal.¹⁰ At parton level, this choice agrees with the Monte Carlo truth with roughly 2/3 accuracy.

Note that in any case we do not use the fourth particle's momentum $p_{t_{\text{miss}}}^\mu$ to reconstruct the vectorlike top.

For the signal regions SR1 and SR2, about a few percent, 30% and 70% of signal events fall in categories (a), (b) and (c), respectively.

5. Results

Event numbers under the cuts described above are shown in Table 2 for all signal regions. All numbers are rescaled to an integrated luminosity of 100 fb^{-1} for the

⁷The parameters are the same as in the BDRS Higgs tagger [12].

⁸We investigated this option and found improved purity and slightly better signal-to-background ratios. It should be considered once higher integrated luminosity is available.

⁹The case of two tops and one Higgs (SR2) proceeds analogously.

¹⁰In our algorithm, we try to avoid any bias on the reconstructed mass. Once the order of the vectorlike top mass is known, this criterion can be optimized accordingly.

Process	$t'\bar{t}'$		b.g.	$bb\bar{b}\bar{b}$	$t\bar{t}$	$t\bar{b}b\bar{b}$	$t\bar{t}h$
	800 GeV	900 GeV					
Cross section[fb]	3.75	1.52		2.20×10^6	1.39×10^5	494	25.5
number of events for 100 fb^{-1}							
$H_T \geq 1200 \text{ GeV}$	266	123	14800	5320	9120	373	29.6
$\#b \geq 4$	185	84.6	1560	1240	210	100	8.5
SR1	25.0	11.3	10.3	2.7	2.9	4.2	0.5
SR2	13.0	5.7	5.8	0.7	2.3	2.5	0.3
SR1+SR2	38.0	17.0	16.1	3.4	5.2	6.7	0.8

Table 2: Cross sections and event numbers for an integrated luminosity of 100 fb^{-1} at the LHC with $\sqrt{s} = 14 \text{ TeV}$. Results for the signal are shown separately for two different masses of the vectorlike top, 800 and 900 GeV. The sum of all relevant background processes (“b.g.”) as well as their individual breakdown is given in the right-hand columns. For the definition of the signal regions (SR) see Table 1. In SR3, the number of signal events for 800 GeV turns out to be less than two with almost vanishing backgrounds < 0.35 .

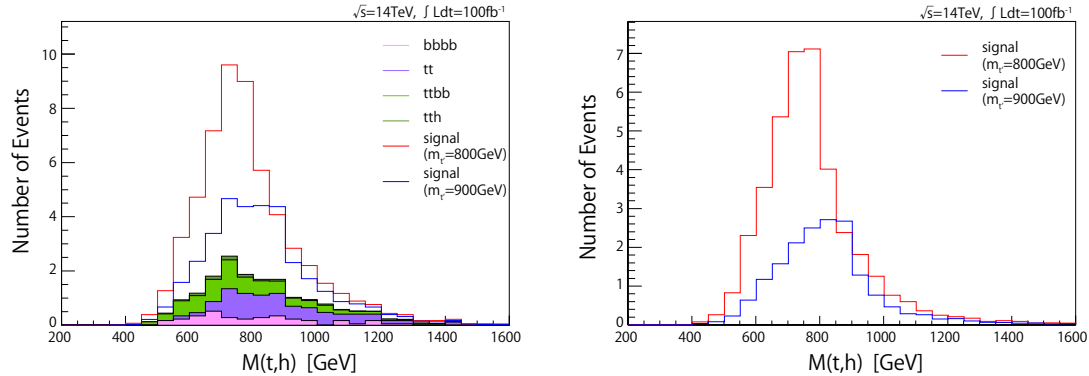


Figure 3: (lhs) The mass distribution of reconstructed vectorlike tops (detector level). The red and blue lines correspond to the signal for different masses of the vectorlike top, $m_{t'} = 800 \text{ GeV}$ and $m_{t'} = 900 \text{ GeV}$, respectively. The black line shows the sum of all relevant background processes; their breakdown is given by the filled curves. Event numbers are stacked. (rhs) The mass distribution for signal events only (detector level).

LHC running at $\sqrt{s} = 14 \text{ TeV}$. We also give cross sections before cuts.¹¹ Signal events are shown for the two model points with $m_{t'} = 800$ and 900 GeV . A breakdown of all considered background processes is given together with their sum (denoted as “b.g.”).

As is evident from Table 2, the first two simple cuts ($H_T \geq 1200 \text{ GeV}$ and $\#b \geq 4$) already drastically suppress the various backgrounds. After top and Higgs tagging and subsequent reconstruction of the vectorlike top, there is a clear excess of signal events over background in both signal regions SR1 ($1t+2h$) and SR2 ($2t+1h$).

For the combined signal region SR1+SR2, the reconstructed mass distribution is given in Fig. 3. The figure shows a clear mass peak of the vectorlike top. For $m_{t'} = 800 \text{ GeV}$, the peak is around 700–800 GeV with a

width of $O(100) \text{ GeV}$ and experiences a steep drop just above the true mass. Falsely-assigned $t\bar{h}$ pairs typically lead to an overestimation of the reconstructed mass. The vanishing low-mass tail in background events is dominated by the cut on scalar transverse momentum H_T . The shape of the peak is also affected by the accuracy of reconstructed tops and Higgs bosons. Tighter mass ranges in the tagging algorithms do lead to a sharper mass peak, but at the cost of decreasing event rates.

For signal events with a vectorlike top mass of 900 GeV the excess over background is smaller. The reconstructed mass peak is lower and wider, but again experiences a sharp edge just above the true mass. A larger cut on scalar transverse momentum (e.g., $H_T \geq 1400 \text{ GeV}$) could further improve the signal-to-background ratio. As the event numbers also drop, this cut should be considered only for larger integrated luminosities.

¹¹See Sec. 3 for event generation and cuts at matrix-element level.

6. Summary and outlook

We investigated fully hadronic final states to search for pair-produced vectorlike top partners at the LHC. Imposing an H_T cut, multibottom cut, and using top/Higgs taggers we can suppress the background processes and reconstruct the vectorlike top. For this reconstruction we proposed an algorithm to determine the t - h combination based on a massive pair hypothesis. We note that our analysis procedure is kept general and in particular not tailored to any model parameter or mass scale except for the initial H_T cut. It was found that the vectorlike top can be reconstructed with good quality and signal-to-background ratio if $\text{BR}(t' \rightarrow th)$ is large.

Although we considered fully hadronic final states, our algorithm can be applied to events with semileptonically decaying vectorlike top quarks as well.

In this article we assumed $\text{BR}(t' \rightarrow th) = 1$. A complete analysis should also cover the cases of generic branching fractions to other possible final states such as $t' \rightarrow bW$ and $t' \rightarrow tZ$. The former decay leads to quite distinct final states, but the latter one can lead to similar event topologies as the $th\bar{h}$ final states, which affects the result of our analysis. Even without considering mistags, the decay chain $t'\bar{t}' \rightarrow (th)(\bar{t}Z)$ can give a contribution to SR2. This will lead to a wrong assumption on the untagged particle's mass when determining the t - h combination from Eqs. (8) and (9). On the other hand, due to the loose mass constraints employed in the Higgs boson tagging algorithm, misidentification of Z as h leads to a broadened mass peak for the vectorlike top. Its shape may act as a handle on determining the correct branching fractions, in conjunction with event counts. As we only give a proof of concept here, a detailed analysis is left for future studies.

Acknowledgment

The speaker is grateful to Motoi Endo, Koichi Hamaguchi, and Kazuya Ishikawa for collaboration. This work was supported by the Program for Leading Graduate Schools, and closely follows Ref. [29].

References

- [1] G. Aad, et al., Observation of a new particle in the search for the Standard Model Higgs boson with the ATLAS detector at the LHC, *Phys.Lett. B*716 (2012) 1–29.
- [2] S. Chatrchyan, et al., Observation of a new boson at a mass of 125 GeV with the CMS experiment at the LHC, *Phys.Lett. B*716 (2012) 30–61.
- [3] N. Arkani-Hamed, A. G. Cohen, H. Georgi, Electroweak symmetry breaking from dimensional deconstruction, *Phys.Lett. B*513 (2001) 232–240.
- [4] M. Schmaltz, D. Tucker-Smith, Little Higgs review, *Ann.Rev.Nucl.Part.Sci.* 55 (2005) 229–270.
- [5] T. Moroi, Y. Okada, Upper bound of the lightest neutral Higgs mass in extended supersymmetric Standard Models, *Phys.Lett. B*295 (1992) 73–78.
- [6] S. Chatrchyan, et al., Inclusive search for a vector-like T quark with charge $\frac{2}{3}$ in pp collisions at $\sqrt{s} = 8$ TeV, *Phys.Lett. B*729 (2014) 149–171.
- [7] ATLAS Collaboration, ATLAS-CONF-2013-018.
- [8] ATLAS collaboration, ATLAS-CONF-2013-051.
- [9] ATLAS collaboration, ATLAS-CONF-2013-056.
- [10] ATLAS collaboration, ATLAS-CONF-2013-060.
- [11] CMS Collaboration, CMS-PAS-B2G-14-002.
- [12] J. M. Butterworth, A. R. Davison, M. Rubin, G. P. Salam, Jet substructure as a new Higgs search channel at the LHC, *Phys.Rev.Lett.* 100 (2008) 242001.
- [13] T. Plehn, M. Spannowsky, M. Takeuchi, D. Zerwas, Stop Reconstruction with Tagged Tops, *JHEP* 1010 (2010) 078.
- [14] J. Beringer, et al., Review of Particle Physics (RPP), *Phys.Rev. D*86 (2012) 010001.
- [15] J. Alwall, M. Herquet, F. Maltoni, O. Mattelaer, T. Stelzer, MadGraph 5 : Going Beyond, *JHEP* 1106 (2011) 128.
- [16] T. Sjostrand, S. Mrenna, P. Z. Skands, PYTHIA 6.4 Physics and Manual, *JHEP* 0605 (2006) 026.
- [17] J. de Favereau, et al., DELPHES 3, A modular framework for fast simulation of a generic collider experiment, *JHEP* 1402 (2014) 057.
- [18] M. L. Mangano, M. Moretti, F. Piccinini, M. Treccani, Matching matrix elements and shower evolution for top-quark production in hadronic collisions, *JHEP* 0701 (2007) 013.
- [19] M. Worek, NLO mass effects in b anti-b b anti-b production at the LHC, *PoS RADCOR2013* (2013) 038.
- [20] N. Kidonakis, R. Vogt, The Theoretical top quark cross section at the Tevatron and the LHC, *Phys.Rev. D*78 (2008) 074005.
- [21] G. Bevilacqua, M. Czakon, C. Papadopoulos, R. Pittau, M. Worek, Assault on the NLO Wishlist: pp $\rightarrow t$ anti-t b anti-b, *JHEP* 0909 (2009) 109.
- [22] R. Frederix, S. Frixione, V. Hirschi, F. Maltoni, R. Pittau, et al., Scalar and pseudoscalar Higgs production in association with a top-antitop pair, *Phys.Lett. B*701 (2011) 427–433.
- [23] M. Cacciari, G. P. Salam, G. Soyez, The Anti-k(t) jet clustering algorithm, *JHEP* 0804 (2008) 063.
- [24] M. Cacciari, G. P. Salam, G. Soyez, FastJet User Manual, *Eur.Phys.J. C72* (2012) 1896.
- [25] ATLAS Collaboration, ATLAS-CONF-2012-043.
- [26] Y. L. Dokshitzer, G. Leder, S. Moretti, B. Webber, Better jet clustering algorithms, *JHEP* 9708 (1997) 001.
- [27] M. Wobisch, T. Wengler, Hadronization corrections to jet cross-sections in deep inelastic scattering, *arXiv:hep-ph/9907280*.
- [28] T. Plehn, M. Spannowsky, Top Tagging, *J.Phys. G*39 (2012) 083001.
- [29] M. Endo, K. Hamaguchi, K. Ishikawa, M. Stoll, Reconstruction of Vector-like Top Partner from Fully Hadronic Final States, *Phys.Rev. D*90 (2014) 055027.